Neutron spectroscopy of aluminium trihydride

1996 J. Phys.: Condens. Matter 8 2529

(http://iopscience.iop.org/0953-8984/8/15/004)

J. Phys.: Condens. Matter **8** (1996) 2529–2538. Printed in the UK

Neutron spectroscopy of aluminium trihydride

A I Kolesnikov†, M Adams‡, V E Antonov†, N A Chirin†, E A Goremychkin§, G G Inikhova†, Yu E Markushkin†, M Prager‖ and I L Sashin§

† Institute of Solid State Physics of the Russian Academy of Science, 142432 Chernogolovka, Moscow District, Russia

‡ Rutherford Appleton Laboratory, Chilton, Didcot, Oxon OX11 0QX, UK

§ Frank Laboratory of Neutron Physics, Joint Institute for Nuclear Research, 141980 Dubna, Moscow District, Russia

‖ Institut für Festkörperforschung, Forschungszentrum Jülich, D-52425 Jülich, Germany

Received 3 January 1996

Abstract. The lattice dynamics of α-AlH_3 and α-AlD_3 were studied by inelastic neutron scattering (INS). The hydrogen optic modes in the INS spectra were shown to form a broad structured band which exhibited an harmonic isotopic behaviour. In contrast, the low-energy part of the phonon spectra, formed mainly by the vibrations of the metal atoms, showed pronounced anharmonicity. The temperature dependence of the AlH_3 heat capacity derived from the INS data agrees with the available experimental dependence at 50–150 K.

1. Introduction

The crystal structure of α-AlH_3, schematically shown in figure 1, essentially differs from the structures of other metal hydrides. It has the trigonal space group $R\bar{3}c$ and six AlH_3 molecules in a hexagonal unit cell with the dimensions $a = 4.449$ Å and $c = 11.804$ Å [1]. The structure consists of alternating planes of Al and H atoms stacked perpendicular to the c axis and spaced at distance $c/12$. Columns of Al atoms and spirals of H atoms are parallel to the c axis and form a three-dimensional network of Al···H···Al bridges. All Al–H nearest distances are 1.715 Å and the shortest Al–Al distances are 3.236 Å.

Any given hydrogen atom in aluminium trihydride has therefore only two nearest metal neighbours and does not occupy any symmetrical interstitial position in the metal sublattice as it does in most other hydrides (for example, in the hydrides of transition and rare earth metals hydrogen usually occupies octahedral and/or tetrahedral interstitial positions [2]). One could thus expect that the lattice dynamics of α-AlH_3 should also have some distinguishing features. In particular, due to rather large Al–Al distances and the Al–Al bonding involving the hydrogen atom, the low-energy 'lattice' part of the phonon spectrum should be noticeably influenced by the hydrogen vibrations.

The present paper reports on the measurement of phonon spectra of α-AlH_3 and α-AlD_3 by using the inelastic neutron scattering (INS) techniques. The sample of aluminium deuteride was contaminated with protium, and its INS spectrum was measured only roughly in order to better understand some characteristic features of the AlH_3 spectrum.

0953-8984/96/152529+10$19.50

2. Experimental details and data treatment

The aluminium hydride powder with a grain size of 30–40 μm and a purity of 99.8 wt% was prepared by a reaction of $LiAlH_4$ with $AlCl_3$ in ether solution at room temperature [3]. The aluminium deuteride powder with a grain size of 20 μm was prepared in the same way using the deuterium-substitued reagents. The main impurity in the deuteride was protium and the H/(H+D) atomic ratio made up $1.5 \pm 0.5\%$ according to the spectral analysis.

The INS spectrum of a 1 g sample of AlH_3 was measured at 25 K using the time-focused crystal analyser (TFXA) spectrometer [4] at the spallation neutron source, ISIS, Rutherford Appleton Laboratory, UK. The spectrometer provided an excellent resolution, $\Delta\omega/\omega \leqslant 2\%$, in the range of energy transfer from 2 to 500 meV. The measured data were transformed to the dynamical structure factor $S(Q, \omega)$ versus energy transfer using standard programs (ω and Q are the neutron energy and the momentum transfer, respectively).

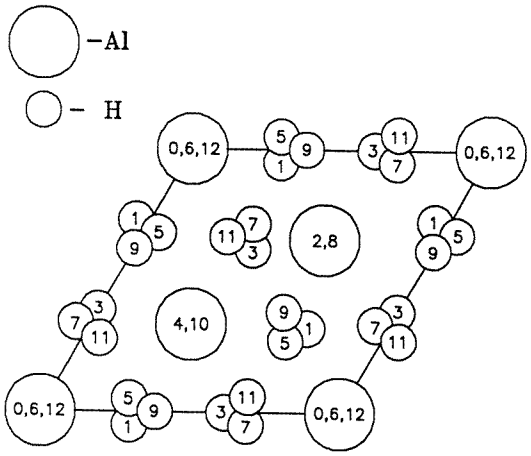

Figure 1. Aluminium trihydride structure as seen in the (001) projection of a hexagonal unit cell. Numbers give the z position of atoms in units of a twelfth of the unit cell dimension c.

The INS experiment on a 15 g sample of aluminium deuteride was carried out at 80 K using the inverted geometry time-of-flight spectrometer KDSOG-M [5] installed at the IBR-2 pulse reactor in Dubna, Russia. The spectrometer has a very high neutron flux at the sample position and provided a medium resolution $\Delta\omega/\omega \simeq 4$–10% in the studied range of energy transfer from 1 to 200 meV. The data were transformed to the generalized vibrational density of states $G(\omega)$ that is a standard procedure at the KDSOG-M spectrometer.

In both cases, a background spectrum determined in a separate empty-can measurement under the same conditions was then subtracted from the obtained experimental spectrum.

The contributions from the multi-phonon neutron scattering (up to four-phonon processes) were calculated in an harmonic isotropic approximation by the multiconvolution of the one-phonon spectrum using an iterative technique [6]. Experimental data in the energy range of the lattice and hydrogen optic modes (the spectra in this range were normalized to $1/m$, where m is the mass of hydrogen or deuterium atom) were used at the first iterative step as the one-phonon spectrum. At the second and subsequent steps, the one-phonon spectrum was assumed to be the difference between the experimental one and that resulting from the calculated multi-phonon spectra (also normalized to $1/m$). The convergence was

reached in three iterations for both experimental spectra.

To take account of higher-order multi-phonon contributions, from $p = 5$ to 20, the Sjölander approximation was used [7]. This approximation is based on the fact that by convoluting p times an arbitrary form function of energy, we obtain at large p a Gaussian (central limit theorem of probability theory) with a mean value E and a variance Δ, which are p times larger than the mean value and variance of the energy for the initial function. The calculations using the Sjölander approximation take a much shorter computer time as compared with the method from [6] and give similar results for large p, especially if E and Δ are of the same order of magnitude (in the case of aluminium trihydride, $E = 86$ meV and $\Delta = 33$ meV).

3. The INS spectrum of AlH_3

The experimental INS spectrum $S(Q, \omega)$ for the AlH_3 sample is shown in figure 2. The spectrum mainly results from neutron scattering on the hydrogen atoms because of the much higher scattering cross section of H atoms than of Al atoms. The measured interval of energy transfer can be divided to three ranges: (i) the lower energy range, 0–44 meV, presumably associated with in-phase vibrations of hydrogen atoms with heavier metal atoms ('lattice vibrations'); (ii) the range 62–131 meV of hydrogen optic modes and (iii) the range above 131 meV of multi-phonon processes.

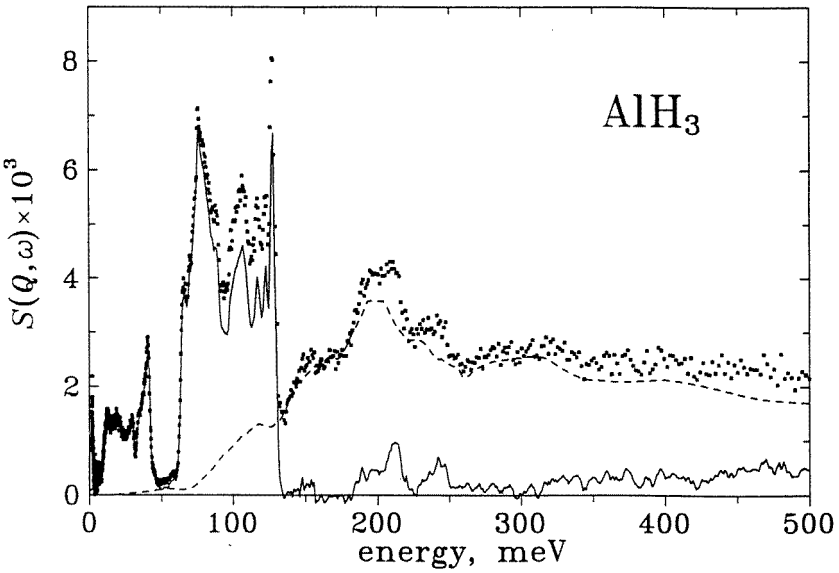

Figure 2. The INS spectrum $S(Q, \omega)$ of AlH_3 (points) measured at TFXA at a sample temperature $T = 25$ K. The calculated multi-phonon contributions are shown as a dashed line. The solid line is the difference between the experimental data and the calculated multi-phonon spectrum.

As is seen from figure 2, the calculated line for the multi-phonon neutron scattering satisfactorily describes the measured spectrum at $\omega > 131$ meV. A certain discrepancy in the calculated and measured intensities is most probably due to the use of an isotropic approximation in the calculations for vibrations of hydrogen atoms whereas these vibrations

are very likely to be essentially anisotropic. At $\omega < 131$ meV, the contribution from the one-phonon scattering is dominant, and the error in its determination (as the difference between the experimental and multi-phonon spectra) is of the order of the experimental error.

The experimental INS spectrum and calculated one- and multi-phonon spectra were transformed to the generalized vibrational density of states (GVDS) according to

$$G(\omega) = \frac{S(Q,\omega)\omega}{Q^2[n(\omega)+1]} \tag{1}$$

where $n(\omega)$ is the Bose factor. The results are shown in figure 3.

As is seen from figure 3, the obtained one-phonon spectrum has a rather intensive 'lattice' part and sharp low-energy and high-energy cutoffs of the hydrogen optic band. Both features are not characteristic of the phonon spectra of hydrides of other metals, for example, those of V, Nb, Pd, Ti, Zr, Ce, La, Pr, Nd and Y with different hydrogen contents, from H/Me = 0.5 to 3, see [2].

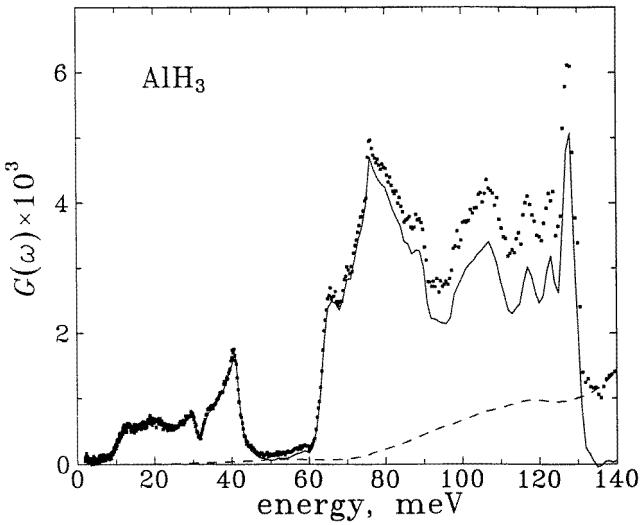

Figure 3. The GVDS $G(\omega)$ of AlH_3 derived from the $S(Q,\omega)$ experimental data (points), the multi-phonon (dashed line) and the one-phonon (solid line) spectra.

The optic band in the one-phonon spectrum of AlH_3 is rather broad, about 70 meV. As the positions of all hydrogen atoms in the crystal structure of AlH_3 are crystallographically equivalent [1], the large width of the optic band suggests a large dispersion of the hydrogen optic phonon branches and, consequently, large H–H force constants. On the other hand, five peaks are clearly seen in the band (with maxima at 76, 104.7, 117.4, 122.9 and 127.6 meV) and the three rightmost of them are very narrow which is indicative of the presence of corresponding phonon branches with almost no dispersion.

The high intensity of the 'lattice' part of the AlH_3 spectrum indicates that the eigenvectors of hydrogen atoms are large for these modes and the 'lattice' phonons should be strongly mixed with the hydrogen optic modes [8].

In the 'lattice' region, there are three small peaks at 12.8, 18.9 and 29.5 meV and one strong peak at 40.5 meV with a shoulder at 34.5 meV. The rightmost peak was positioned rather high in energy and its intensity was large, so it was not clear whether the peak

originated from aluminium modes or not. In fact, the rightmost peak in the GVDS spectrum of pure aluminium is observed at lower energy, about 35 meV [9], though the shortest Al–Al distance in aluminium metal is 13% smaller than in AlH_3, so one could rather expect the opposite effect. On the other hand, this 40.5 meV peak in the AlH_3 spectrum might be either a split part of the usual hydrogen optic vibrations or, for example, some kind of a resonant-like hydrogen mode in the range close to 'lattice vibrations' of the metal atoms, similar to those observed in $NbH_{0.05}$ [10].

4. The INS spectrum of AlD_3

A prospective means for better understanding the nature of the peak in question was the investigation of the GVDS spectrum of AlD_3, because the parts of the AlD_3 and AlH_3 spectra which correspond to the hydrogen optic modes should exhibit nearly harmonic isotopic behaviour and hence should nearly coincide if the spectrum of AlH_3 is plotted as a function of

$$\omega = \omega_{\mathrm{exp}}/\sqrt{m_{\mathrm{D}}/m_{\mathrm{H}}} \approx \omega_{\mathrm{exp}}/\sqrt{2}.$$

The points in figure 4 represent the GVDS of aluminium trideuteride as measured on the KDSOG-M spectrometer. One can see that the shape of this experimental spectrum, $G_{\mathrm{exp}}(\omega)$, essentially differs from the curve (d) representing $G(\omega)$ for AlD_3. Curve (d) was calculated in an harmonic approximation using the experimental $G(\omega)$ of AlH_3 (shown partly with points in figure 3) which was smoothed to allow for the different resolutions of the TFXA and KDSOG-M spectrometers (this smoothed spectrum is referred to as $G_{\mathrm{AlH_3}}(\omega)$ hereinafter). The difference between the curves (a) and (d) in the range of deuterium optic vibrations and multi-phonon processes ($\omega > 42$ meV) was obviously due to the neutron scattering on approximately 1.5% of protium contained in the sample of aluminium trideuteride. This contribution from the protium atoms was estimated by minimizing the integral

$$I(n_1, n_2) = \int \left[G_{\mathrm{exp}}(\omega) - n_1 \cdot G_{\mathrm{AlH_3}}(\omega) - n_2 \cdot G_{\mathrm{AlH_3}}(\omega/\sqrt{2}) \right]^2 \mathrm{d}\omega \qquad (2)$$

where integration was taken over the interval 42 to 140 meV and n_1 and n_2 were the parameters to be determined.

The obtained values of n_1 and n_2 were used to plot the calculated spectra for the AlH_3 and AlD_3 constituents of the studied aluminium deuteride (figure 4, curves (b) and (d)). The 'experimental' spectrum of AlD_3 (curve (c)) was then determined by subtracting the contribution of AlH_3, curve (b), from curve (a).

The hydrogen content of the studied aluminium trideuteride estimated from the ratio of the intensities of the calculated hydrogen (curve (b)) and deuterium (curve (d)) optic bands was equal to 1.3% which agreed with the value of 1.5 ± 0.5% given by the spectral analysis. The hydrogen optic band of the 'experimental' spectrum of AlD_3, curve (c), was similar to that calculated in the harmonic approximation, curve (d) (the low-energy cutoffs were exactly the same, the positions of the maxima of the main peaks were also close to each other). These facts suggest that the protium atoms in the studied trideuteride formed large clusters, because in the case of protium atoms being randomly distributed over the sample volume their vibrational spectrum would noticeably differ from the spectrum of AlH_3 crystal.

The one-phonon spectrum of AlD_3 derived from the 'experimental' spectrum (figure 4, curve (c)) is shown in figure 5 by curve (c). The peak corresponding to one observed at

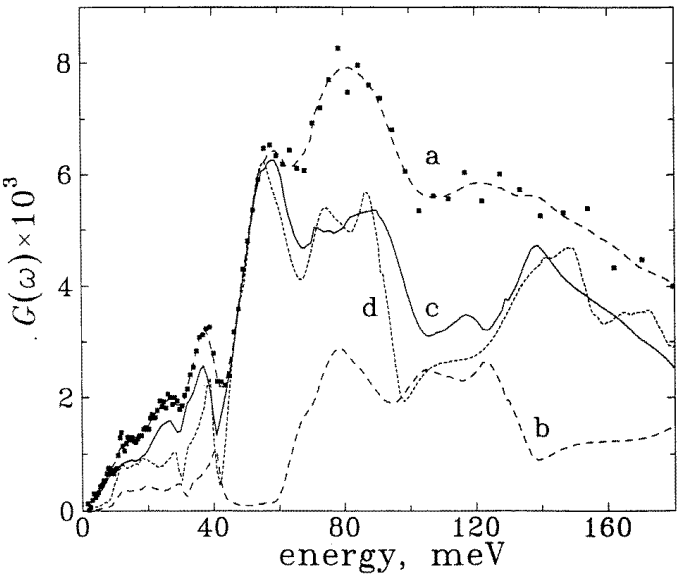

Figure 4. The GVDS for aluminium deuteride: (a) the $G_{\rm exp}(\omega)$ spectrum as measured on the KDSOG-M at 80 K; (b) the experimental spectrum of AlH_3 smoothed using the resolution function of the KDSOG-M spectrometer, $G(\omega) = n_1 \cdot G_{AlH_3}(\omega)$; (c) the difference between the curves (a) and (b) considered as the GVDS for pure AlD_3; (d) the calculated spectrum representing the GVDS for pure AlD_3 in an harmonic approximation, $G(\omega) = n_2 \cdot G_{AlH_3}(\omega/\sqrt{2})$ at $\omega \geqslant 42$ meV and $G(\omega) = n_2 \cdot G_{AlH_3}(\omega/\sqrt{33/30})$ at $\omega < 42$ meV. The coefficients n_1 and n_2 are from equation (2).

40.5 meV in the spectrum of AlH_3 (figure 3) is now at 37 meV. The ratio $40.5/37 \approx 1.095$ for the positions of these peaks is much closer to the square root of the 'molecular' mass ratio

$$\sqrt{m_{AlD_3}/m_{AlH_3}} \approx \sqrt{33/30} \approx 1.049$$

than to square root of the mass ratio for hydrogen isotopes,

$$\sqrt{m_D/m_H} \approx \sqrt{2} \approx 1.41.$$

The peaks should therefore be ascribed to the 'lattice' modes.

In order to compare the low-energy parts of the $G(\omega)$ spectra for AlD_3 and AlH_3, the latter was plotted in figure 4 as a function of $\omega/\sqrt{33/30}$ at $\omega < 42$ meV. As is seen, the 'lattice' parts of the AlD_3 and AlH_3 phonon spectra, curves (c) an (d), are noticeably different. To account for this difference, one needs to admit that the corresponding force constants (presumably, those of Al–Al interactions) responsible for the 'lattice' modes in AlD_3 are smaller than in AlH_3. The observed softening of the 'lattice' modes in AlD_3 is a little surprising because interatomic distances in AlD_3 are smaller than in AlH_3 (the lattice parameters are $a = 4.431$ Å, $c = 11.774$ Å for the deuteride and $a = 4.449$ Å, $c = 11.804$ Å for the hydride [1]) which usually results in an increase of interatomic forces. It is worth noting, however, that there is no energy gap between the 'lattice' and hydrogen optic modes in the spectrum of AlD_3, while such a gap exists in the case of AlH_3 (compare figures 3 and 5). The overlapping of these 'lattice' and optic modes can result in their strong interaction which manifests itself in the softening of the 'lattice' modes in AlD_3.

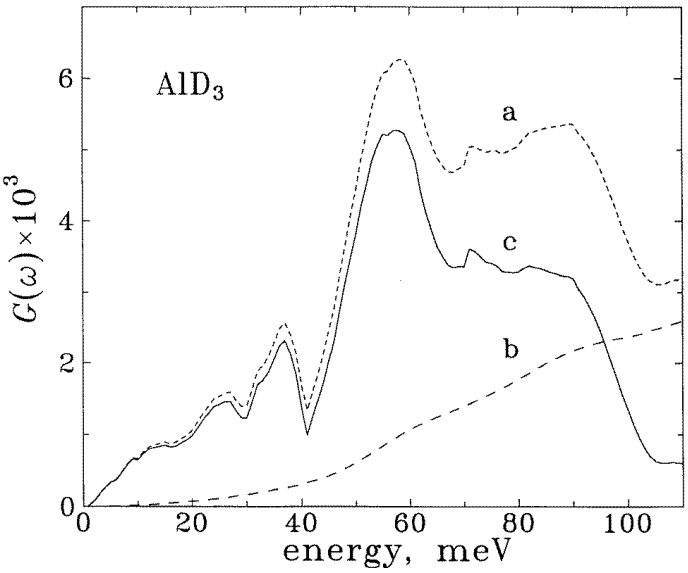

Figure 5. The GVDS of AlD_3: (a) derived from the experimental spectrum (curve (c) in figure 4); (b) the multi-phonon contributions; (c) the one-phonon spectrum (the difference between the curves (a) and (b)).

5. The heat capacity of AlH_3 and AlD_3

The heat capacity at constant pressure, C_p, of AlH_3 was studied experimentally within the temperature interval 30–298 K [11]. Aluminium trihydride is dielectric and its heat capacity is determined by the density of phonon states, $g(\omega)$. We estimated $g(\omega)$ from the measured $G(\omega)$ and used it to calculate the lattice heat capacity at constant volume, $C_v(T)$, to be compared with the experimental $C_p(T)$.

The $g(\omega)$ spectrum was derived from $G(\omega)$ as follows. Firstly, the one-phonon $G(\omega)$ spectrum (figure 3, solid line) was divided by the Debye–Waller factor, $\exp\left(-\langle u_H^2\rangle Q^2\right)$, where the value for hydrogen mean-square displacement, $\langle u_H^2\rangle = 0.024$ Å^2, was estimated from the experimental $G(\omega)$ in a standard way [2]. Secondly, under the usual assumptions [12] that $g(\omega) \propto G(\omega)$ in the 'lattice' part of the vibrational spectrum and that the squares of the hydrogen eigenvectors of the 'lattice' and hydrogen optic modes are different, but energy independent, the areas under the 'lattice' and hydrogen optic parts of the spectrum were normalized to 18 and 54 states in accordance with the number of corresponding modes.

The obtained $g(\omega)$ is plotted in figure 6, curve (a). The heat capacity was calculated as

$$C_v(T) = k_B \int \left(\frac{\omega}{k_B T}\right)^2 g(\omega)\, n(\omega)\, [n(\omega)+1]\, \mathrm{d}\omega \qquad (3)$$

where $g(\omega)$ was assumed to be temperature independent.

The calculated $C_v(T)$ is shown in figure 7 as a solid line. The fitting of this dependence to a T^3 form at $T \leqslant 15$ K gave a value of 471 K for the Debye temperature of AlH_3.

As is seen from figure 7, the calculated $C_v(T)$ curve agrees well with the experimental $C_p(T)$ data from [11] at temperatures from 50 to 150 K. At higher temperatures, however, it goes noticeably higher, though one could rather expect the opposite relation between C_v

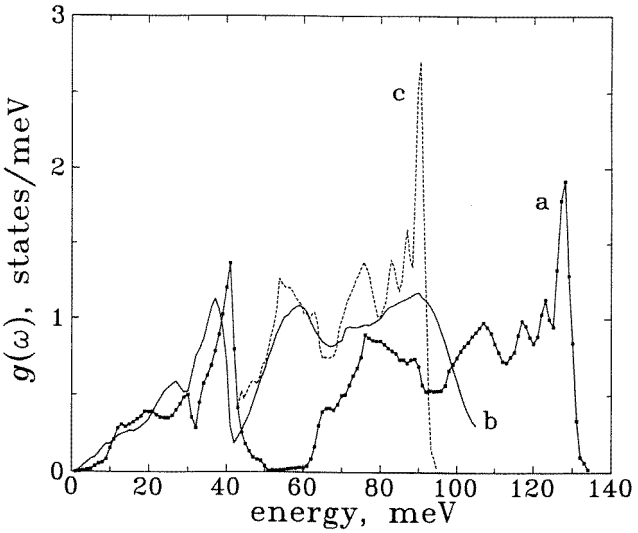

Figure 6. The density of phonon states $g(\omega)$ of AlH_3 (a) and AlD_3 (b) obtained from the experimental one-phonon $G(\omega)$ spectra. The dashed curve shows the hydrogen optic band for AlD_3 derived from $g(\omega)$ of AlH_3, curve (a), in the harmonic approximation.

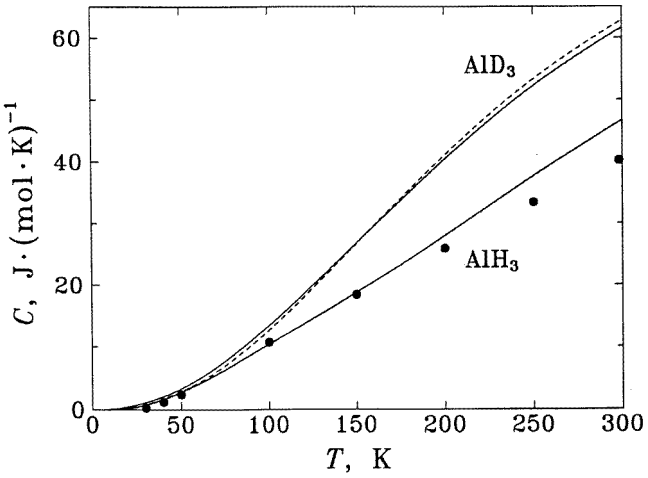

Figure 7. Temperature dependences of heat capacities, $C(T)$. The points show the experimental $C_p(T)$ for AlH_3 [11]. The lower and upper solid lines represent $C_v(T)$ for AlH_3 and AlD_3 calculated according to equation (3) from the 'experimental' phonon density of states (curves (a) and (b) in figure 6). The dashed line depicts $C_v(T)$ for AlD_3 calculated using the phonon spectrum represented by curve (c) in figure 6.

and C_p. This disagreement, along with the errors resulting from the approximations used to calculate C_v, might also be due to the low purity, about 95 wt%, of the AlH_3 sample measured in [11].

Similar calculations were also carried out for AlD_3. The $g(\omega)$ spectrum of AlD_3 derived from the one-phonon $G(\omega)$ spectrum (figure 5, curve (c)) is presented in figure 6, curve

(b). The calculated $C_v(T)$ dependence is shown in figure 7 as a solid line.

As the obtained INS data for AlD_3 were not very reliable, especially in the region of 'lattice' vibrations, we decided to test the response of the calculated $C_v(T)$ dependence to changes in the $g(\omega)$ spectrum. For this purpose, a new $g(\omega)$ spectrum (figure 6, curve (c)) was composed for AlD_3. It had the same 'lattice' part as the AlH_3 spectrum (curve (a) at $\omega < 42$ meV) whereas its hydrogen optic band (the dashed line at $\omega \geqslant 42$ meV) was obtained from that of the AlH_3 spectrum in the harmonic approximation, i.e. the data for AlH_3 were plotted as a function of $\omega = \omega_{exp}/\sqrt{2}$ and normalized so that the area under the curve was equal to 54 states.

The $C_v(T)$ dependence for AlD_3 calculated using this compound $g(\omega)$ is shown in figure 7 as a dashed line. At low temperatures, below about 50 K, where the contribution from the 'lattice' vibrations is dominant, this dependence practically coincides with the dependence for AlH_3 because they were both calculated using the same 'lattice' part of $g(\omega)$. At higher temperatures, the contribution from the hydrogen optic vibrations begins to dominate the 'lattice' one, and the difference between the two $C_v(T)$ dependences calculated for AlD_3 does not exceed a few per cent within the temperature interval 100–300 K.

One could hardly expect that more accurate INS measurements would result in a $g(\omega)$ spectrum of AlD_3 which deviates from curve (b) much more than curve (c) does. So, in the framework of the approximations used, the curves for AlD_3 in figure 7 should satisfactorily represent its heat capacity at moderate temperatures.

6. Conclusions

As aluminium trihydride is thermodynamically unstable under normal conditions [3] and can hardly be prepared in the form of a large enough single crystal, the powder INS data are most informative for modelling its lattice dynamics. The INS spectrum of AlH_3 was measured in the present work with resolution and statistics sufficient to reveal rather strong and narrow peaks in both 'lattice' and hydrogen optic bands, see figure 3, which is very helpful in finding reliable force constants etc. The AlH_3 crystal, however, has 24 atoms in the unit cell, so the total number of phonon modes is 72. This is too many for constructing an unambiguous model on the basis of the available INS data.

The necessary additional information about the lattice dynamics of AlH_3 might be obtained from the INS investigations at high pressures. According to the x-ray and neutron diffraction data [13, 14], the crystal lattice of aluminium trihydride (figure 1) contracts mainly in the basal plane as the pressure increases. All Al–H nearest distances and the H–H nearest distances between hydrogens in different planes remain approximately unchanged, whereas the H–H distances between neighbouring hydrogens belonging to one plane decrease and approach those for hydrogens in different planes. The data of high pressure INS measurements will thus allow the tracing of the effect of changing some interactions with the others being fixed. The experiment is in progress now.

Acknowledgments

We thank the SERC for access to the ISIS pulsed neutron source. This work has been supported in part by the grant no REP300 from the International Science Foundation and the Russian Government and by the grant no 96-02-17522 from the Russian Foundation for Fundamental Research. One of us (AIK) would like to thank Institut für Festkörperforschung des Forschungzentrum Jülich for the financial support and hospitality during his stay there.

References

[1] Turley J W and Rinn H W 1969 *Inorg. Chem.* **8** 18–22
[2] Gel'd P V, Ryabov R A and Mokhracheva L P 1985 *Hydrogen and Physical Properties of Metals and Alloys* (Moscow: Nauka) p 232 (in Russian)
[3] Brower F M, Matzek N E, Reigler P F, Rinn H W, Roberts C B, Schmidt D L, Snover J A and Terada K 1976 *J. Amer. Chem. Soc.* **98** 2450–3
[4] Penfold J and Tomkinson J 1986 *Rutherford Appleton Laboratory Internal Report No* RAL-86–019
[5] Belushkin A V (ed) 1991 *User Guide: Neutron experimental facilities at JINR* (Dubna: JINR) 72
[6] Antonov V E, Belash I T, Kolesnikov A I, Mayer J, Natkaniec I, Ponyatovskii E G and Fedotov V K 1991 *Sov. Phys. Solid State* **33** 87–90
[7] Sjölander A 1958 *Arkiv för Fysik* **14** 315–71
[8] Dorner B, Bokhenkov E L, Chaplot S L, Kalus J, Natkaniec I, Pawley G S, Schmezer U and Sheka E F 1982 *J. Phys. C: Solid State Phys.* **15** 2353–65
[9] Chevrier J, Suck J B, Capponi J J and Perroux M 1988 *Phys. Rev. Lett.* **61** 554–7
[10] Lottner V, Schober H R and Fitzgerald W J 1979 *Phys. Rev. Lett.* **42** 1162–5
[11] Sinke G C, Walker L C, Oettings F L and Stull D R 1967 *J. Chem. Phys.* **47** 2759–61
[12] Springer T and Richter D 1987 *Methods of Experimental Physics* ed K Sköld and D Price (New York: Academic Press) 131–86
[13] Baranowski B, Hochheimer H D, Strössner K and Hönle W 1985 *J. Less-Common Metals* **113** 341–7
[14] Goncharenko I N, Glazkov V P, Irodova A V and Somenkov V A 1991 *Physica* B **174** 117–20